The single-jet inclusive cross-section and its definition

Matteo Cacciari[a,b] , **Stefano Forte**[c] , **Davide Napoletano**[d] , **Gregory Soyez**[d] and **Giovanni Stagnitto**[a,b,c]

[a] *Université Paris Diderot, F-75013 Paris, France*

[b] *Sorbonne Université, CNRS, Laboratoire de Physique Thórique et Hautes Énergies, LPTHE, F-75005 Paris, France*

[c] *Tif Lab, Dipartimento di Fisica, Università di Milano and INFN, Sezione di Milano, Via Celoria 16, I-20133 Milano, Italy.*

[d] *IPhT, CEA Saclay, CNRS, Université Paris-Saclay, F-91191 Gif-sur-Yvette cedex, France.*

E-mail: cacciari@lpthe.jussieu.fr, forte@mi.infn.it, davide.napoletano@ipht.fr, gregory.soyez@ipht.fr, giovanni.stagnitto@lpthe.jussieu.fr

ABSTRACT: We investigate some well-known problematic aspects of the single-jet inclusive cross-section, specifically its non-unitarity and the possibly related issue of apparent perturbative instability at low orders. We study and clarify their origin by introducing possible alternative weighted definitions of the observable which restore unitarity. We show that the perturbative instability of the standard definition is an accidental artefact of the smallness of the NLO K factor which only manifests itself for values of the jet radius in the range $R \sim 0.3 - 0.6$, and that its non-unitarity is necessary in order to ensure cancellation of logs of the momentum cutoff used in the jet definition. We also show that alternative unitary definitions do not have better perturbative properties compared to the conventional non-unitary definition, while suffering from lack of cancellation of large logs.

Contents

1 Introduction

The single-jet inclusive cross-section has been used for now over thirty years [1] for the determination of parton distributions. As an observable, it is defined in a deceptively simple way [2, 3]: count all jets which fall in any given kinematic bin and add them up. While this definition is remarkably simple, a minutes' reflection shows that it has a somewhat peculiar and perhaps undesirable feature. Namely, it is not unitary: each event is counted more than once, so that the integral of the differential cross-section does not yield the total cross-section. The recent computation of the next-to-next-to-leading order (NNLO) corrections to this observable [4, 5] has shown another seemingly problematic aspect: the scale dependence of the result is not significantly reduced and the size of the K factor does not significantly decrease when going from NLO to NNLO, at least with certain scale choices, which suggests a possible perturbative instability.

In Ref. [5] the perturbative properties of this observable were extensively studied, in particular by a numerical analysis of the contributions to individual jet bins with a variety of computational setups (such as the choice of scale and of jet radius). Here we approach the problem of understanding the behavior of this observable from a somewhat different point of view: namely, by trying to see how it behaves upon changes of its definition, specifically motivated by an attempt to correct for its non-unitarity. We then study the properties of this family of new, unitary definitions both numerically, and analytically in a simple collinear approximation.

Our main conclusion is that what seems to be an undesirable feature, namely the non-unitarity of the standard definition, automatically guarantees that results are stable upon changes of the cutoff momentum scale used to in order to define a jet, i.e. the minimum momentum that a jet must carry. Introducing an alternative, unitary definition of the cross-section, preserving insensitivity to the momentum cutoff, is nontrivial, and requires that unitarity be made compatible with independence of the number of jets: we will show two examples demonstrating how this could be achieved.

On the other hand, what may appear to be a lack of perturbative convergence when going from NLO to NNLO, with the NNLO correction [5] larger or of the same order of the NLO one, is actually a manifestation of the fact that the NLO correction of the cross-section depends on R in such a way that it changes sign around $R \sim 0.4$, and it is thus accidentally small, with small theoretical uncertainties, around $R = 0.4$. The perturbative properties of alternative, weighted definitions are generally similar to that of the standard definition, though often worse, for reasons closely related to the sensitivity to the transverse momentum cutoff.

The outline of this paper is the following. First, in Sect. 2 we discuss the standard definition of the cross-section and its non-unitarity, and present a family of alternative, unitary definitions. Then, in Sect. 3 we compare results obtained using various definitions at NLO. In Sect. 4 we show how the results of the previous section can be understood in terms of an analytical calculation. Finally, we draw our conclusions in Sect. 5.

2 The single-jet inclusive cross-section and its definition

The single-jet inclusive cross-section is defined in terms of the differential cross-section $\frac{d\sigma_{N\,\mathrm{jets}}}{dp_{t1}\dots dp_{tN}}$ for producing N jets (after cuts) with transverse momenta p_{ti}, as

$$\frac{d\sigma}{dp_t} = \sum_N \frac{d\sigma_{N\,\mathrm{jets}}}{dp_t} \tag{2.1}$$

$$\frac{d\sigma_{N\,\mathrm{jets}}}{dp_t} = \int dp_{t1}\dots dp_{ti}\dots dp_{tN}\,\frac{d\sigma_{N\,\mathrm{jets}}}{dp_{t1}\dots dp_{ti}\dots dp_{tN}} F_N\left[p_{t1},\dots,p_{tN};p_t\right], \tag{2.2}$$

where F_N, for a standard definition, is given by

$$F_N^{\mathrm{std}}\left[p_{t1},\dots,p_{tN};p_t\right] = \sum_{i=1}^{N}\delta(p_{ti}-p_t), \tag{2.3}$$

and it fills the bin with transverse momentum p_t by picking all contributions from the fully differential N-jets cross-section. The sum in Eq. (2.1) runs over the number of jets in each event that pass some kinematic cut. The sum over the total number of jets starts with $N = 1$ (the $N = 0$ case gives of course no contribution) and goes up to two at leading order (LO), three at NLO, and generally $p + 2$ at N^{p}LO.

It is clear that the inclusive-jet cross-section defined in this way is not unitary, in that its integral over p_t does not give the total number of scattering events per unit flux per unit time within a given fiducial region. Indeed, with this definition, when filling a histogram in p_t, an event with N jets is binned N times. This lack of unitarity may be cause of concern: one is used to the fact that the unitarity of the total partonic cross-section is crucial in order to ensure its infrared finiteness, given that infrared singularities cancel between terms with different numbers of final–state partons. On the other hand, infrared finiteness of the N-jet cross-section is ensured by the use of a jet definition, so the question is really whether this definition leads to a good perturbative behavior.

In order to address the question in a quantitative way, we generalize the definition of the single-jet inclusive cross-section by introducing jet weights that render the cross-section unitary. Namely, we modify the definition Eq. (2.2) by introducing weights in the definition of the function F_N, Eq. (2.3):

$$F_N\left[p_{t1},\dots,p_{tN};p_t\right] = \sum_{i=1}^{N}\delta(p_{ti}-p_t)w^{(N)}(p_t;p_{t1},\dots,p_{tN}) \tag{2.4}$$

The choice $w^{(N)} = 1$ represents the standard non unitary definition Eq. (2.3). The choice $w^{(N)} = 1/N$ restores unitarity, but has undesirable discontinuities whenever the kinematics of the final state changes in such a way that the number of jets jumps from N to $N+1$. In this work, we consider a set of weights defined as

$$w^{(N)}(p_t;p_{t1},\dots,p_{tN}) = \begin{cases} 1 & \text{(standard)} \\[2mm] \dfrac{p_t^r}{\sum_{j=1}^{N}p_{tj}^r} & \text{(weighted)} \end{cases} \tag{2.5}$$

where p_{tj} is the transverse momentum of the j-th jet. All weighted choices lead to a unitary definition.

We consider specifically three families of definitions of these weights, according to which jets are included when constructing the weights.

- *A: jets above p_t^{cut}*
  Only jets with $p_t \geq p_t^{\mathrm{cut}}$ are included in the definitions of F_N Eq. (2.4). In particular, this implies that the sum in the denominator of Eq. (2.5) includes only jets for which $p_{tj} \geq p_t^{\mathrm{cut}}$. When $r = 0$ this reduces to the simplest unitary choice with all weights equal to $1/N$.

- *B: all jets*

  F_N includes all the jets but the numerator in the weight definition, Eq. (2.5), only includes jets above p_t^{cut}. In particular, the denominator in Eq. (2.5) sums over all jets. This definition is infrared safe only for $r > 0$. While this definition may seem unphysical, in practice it corresponds to having a p_t^{cut} that is small compared to the p_t value of the first bin one is interested in.

- *C: two leading jets*

  Only the first two leading jets in p_t are included in the definition of both F_N and the weights, so $N = 2$ in both Eqs. (2.4) and (2.5). In this case we consider the two leading jets independently on whether their p_t is larger or smaller than a possible p_t^{cut}.

These definitions are "unitary" in the sense that the weights add up to one. This implies that, with the first definition, integrating over p_t gives the total cross-section to have at least one jet above p_t^{cut}. For the second definition (with $p_t^{\mathrm{cut}} \to 0$ or an explicit underflow bin) and for the third definition, one instead gets the total pp cross-section. To keep the discussion simple, we do not impose any rapidity cut in the studies carried on in this paper. Nevertheless each of the previous definitions could be extended to the case in which a rapidity cut is introduced. Note that in the case of the third definition, a rapidity cut could change what the leading jets are. To avoid potential issues, in particular for $r < 0$ which is more sensitive to small p_t, one might have in practice to impose an additional dijet selection cut (similar to what is already done when studying e.g. the dijet invariant mass).

To highlight the various features we are interested in studying in this work, it is useful to consider different ways of organizing the perturbative calculation of the single-jet inclusive cross-section at N^{p}LO accuracy. This can, in fact, be written as a sum of contributions, each of order α_s^{2+k}, $k = 0, \ldots, p$, assuming that the leading-order (LO) process is of order α_s^2:

$$\frac{d\sigma^{\mathrm{N}^p\mathrm{LO}}}{dp_t} = \sum_{k=0}^{p} \frac{d\sigma^{(k)}}{dp_t}. \tag{2.6}$$

Furthermore, it is useful to think about the order α_s^{k+2} contribution in two different ways. The first is as a sum of contributions with a different number of jets, as we have done in Eq. (2.2). In such a case, the k-th order contribution to the cross-section is built out of terms containing at most $k + 2$ jets i.e. two at LO ($k = 0$), three at NLO ($k = 1$) and so forth:

$$\frac{d\sigma^{(k)}}{dp_t} = \sum_{N=1}^{k+2} \frac{d\sigma^{(k)}_{N\,\mathrm{jets}}}{dp_t}. \tag{2.7}$$

Eq. (2.7) is the same as Eq. (2.1), but for the k-th order contribution only. However, in order to understand the perturbative behavior of the cross-section it also useful to break it up into the contribution from the jet with the largest p_t (leading, or first jet), the jet with the second largest p_t (subleading, or second jet), and so on:

$$\frac{d\sigma^{(k)}}{dp_t} = \sum_{n=1}^{k+2} \frac{d\sigma^{(k)}_{n\text{-th jet}}}{dp_t}. \tag{2.8}$$

In Eq. (2.7), $d\sigma^{(k)}_{N\,\mathrm{jets}}/dp_t$ is the contribution to the cross-section coming from configurations with N jets, while in Eq. (2.8) $d\sigma^{(k)}_{n\text{-th jet}}/dp_t$ is the contribution coming from the n-th leading jet. The range of the sum is the same in both cases and it is equal to the maximum number of jets that can be produced at a given perturbative order k.

3   Comparing definitions of the cross-section

In order to study the effects of the various unitary definitions, Eq. (2.5), we start by simply comparing results obtained in each case for the NLO K factors and individual jet contributions. This way, we can see how

imposing unitarity affects the p_t distribution of the single-jet inclusive cross-section. In Section 4 we then turn to analytic arguments, both in general and in a collinear approximation.

All results presented in this section are obtained using the following setup. Computations up to NLO are performed using `NLOJET++`(v4.1.3) [6, 7] for pp collisions, with center of mass energy $\sqrt{s} = 13$ TeV. Parton distribution functions are taken from the NNPDF3.1 [8] set at NNLO, with $\alpha_s(M_Z) = 0.118$, and interfaced using the `LHAPDF` library (v6.1.6) [9]. Jets are clustered using the anti-k_t algorithm [10], as implemented in `FastJet`(v3.3.2) [11], with $R = 0.4$, unless otherwise specified.

The dependence on the choice of central factorization and renormalization scale (see e.g. the discussion in [5]) is studied by considering three options: (i) the *average dijet scale*,

$$p_t^{(\text{avg})} = \frac{p_{t1}^{(R=1)} + p_{t2}^{(R=1)}}{2}, \tag{3.1}$$

where $p_{t1,2}^{(R=1)}$ are the transverse momenta of the two leading jets clustered with a radius $R = 1$ [12], (ii) the *partonic scalar k_t halved*,

$$\frac{\hat{H}_T}{2} = \frac{1}{2} \sum_{i=1}^{n\text{-partons}} k_{ti}, \tag{3.2}$$

suggested as an optimal scale choice in [5], and (iii) the *leading jet p_t*, $p_t^{(\text{max})}$, defined as p_t of the leading $R = 1$ jet.

For each choice of central scale, uncertainty bands are obtained with the 7-point scale variation rule [13]. As noted in [12] and as we discuss below, the uncertainty bands around the NLO prediction are unnaturally small because of an unphysical cancellations in scale dependence between the production of hard partons, a large angle process, and their fragmentation into jets, a small angle one. A more reliable estimate could be obtained by factoring the cross-section for producing a small-radius jet into the cross-section for the initial partonic scattering and the fragmentation of the parton to a jet, considering separately the uncertainties of these two processes and summing them in quadrature. This option has been studied in [12] and in great details more recently in [14]. In this paper, we have checked the effects of decorrelated scale variation on the weighted definitions, and we briefly comment on this below.

3.1 Standard (non-unitary) definition

We start by discussing some well-known results for the standard definition. As mentioned, we focus on two observables: the total NLO K factor, and the individual n-th-leading jet NLO K factor as a function of p_t,

$$K = \sum_{n=1}^{3} K_n, \quad \text{with} \quad K_n = \frac{d\sigma_{n\text{-th jet}}^{\text{NLO}}}{d\sigma^{\text{LO}}}. \tag{3.3}$$

They are shown in Fig. 1 for the standard definition. Three main features are apparent. First, while the total NLO K factor is quite close to one (see the right plot in Fig. 1), the individual K_n for the leading and subleading jet deviate from their leading order value, $1/2$, by sizable amounts (see the left plot in Fig. 1). However, they almost exactly compensate when added up into the total cross-section, yielding a total NLO K factor close to 1, as well as a scale uncertainty much smaller than those of the individual K_n. This almost exact compensation is largely accidental as it depends on the value of the jet radius. This can be seen in Fig. 2, where we plot the K factor for the total cross-section as a function of R: the leading and the second leading jet K factors only compensate (up to a residual $\sim 10\%$ effect) in the region $R \sim 0.3 - 0.6$. This effect has also been noticed in Refs. [12, 14]. The behavior of the individual jet K factors can be explained in a simple fashion. At NLO, the K factor of the leading jet K_1 is substantially larger than one, most likely a consequence of recoil effects amplified by the fact that the LO cross-section is steeply falling — typically with a power around 5 — in p_t. Furthermore, at NLO, K_1 does not depend on R, as explicitly visible in Fig. 2 and as we show analytically in Sect. 4.1 below. However K_2 decreases at small R since out-of-cone final state radiation depends on the jet radius and has the effect of lowering the p_t of the emitter. This effect is again drastically enhanced by the steeply-falling nature of the LO differential cross-section in p_t.
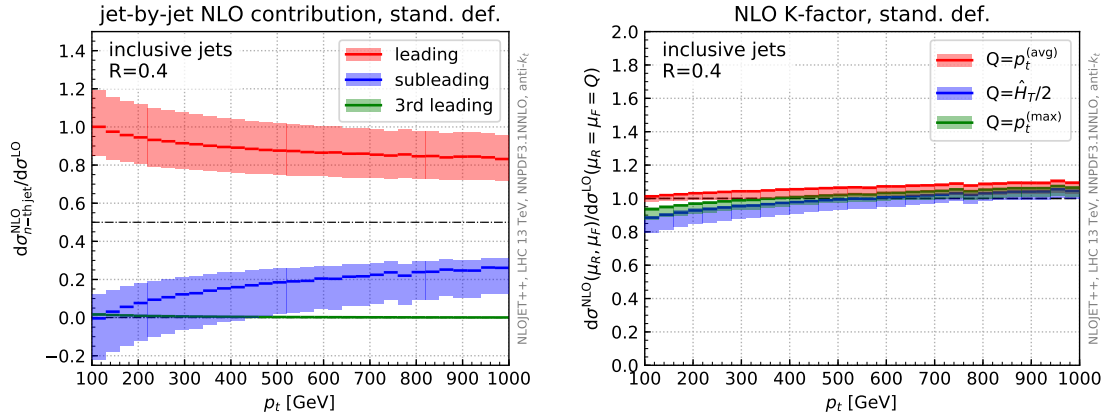
Figure 1. Left: Contributions from the leading, subleading, and third-leading jet to the NLO inclusive cross-section, with central scale choice $\mu_R = \mu_F = p_t^{(\mathrm{avg})}$ Eq. (3.1). Right: Inclusive NLO K factors, with three different central scale choices (see text).
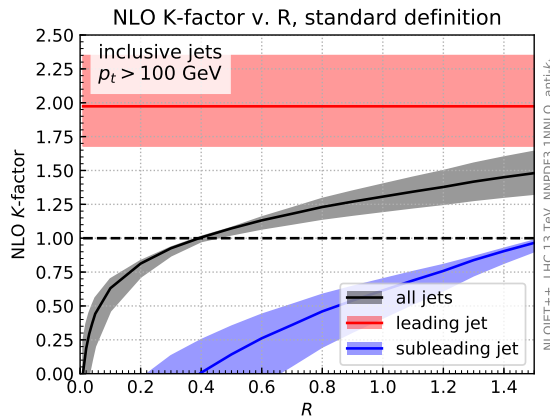

Figure 2. The NLO K factor for the single-inclusive total jet cross-section as a function of the radius R of the jet (black). The contributions from the leading jet (red) and the subleading jet (blue) are also shown.

Second, while the leading and second jet account for most of the cross-section, the contribution of the third jet to the total K factor is much smaller (giving a correction of less than 2% of the LO cross-section) and almost completely negligible. Finally, by inspecting the uncertainty bands shown in Fig. 1, one can see that scale variation bands for $R = 0.4$ for different central scale choices do not overlap in the small p_t region. An in-depth discussion of this problem and how this changes when including even higher order QCD corrections is given in Ref. [5]. It is however clear that this is a consequence of the accidental compensation of the two leading jets discussed above, which then propagates onto the scale variation. It follows that theoretical uncertainties obtained by performing standard scale variation for fixed $R \sim 0.4$ are unrealistically small. A more reliable estimate can be obtained performing uncorrelated scale variation [12, 14], which then leads to overlapping scale uncertainties across the whole p_t spectrum.

All this shows that the putative perturbative instability of the standard definition is in fact a byproduct of an entirely accidental cancellation which happens only at NLO in a given R range. Because this cancellation is not protected by a symmetry, one should not expect it to persist with a different definition or at higher perturbative orders.
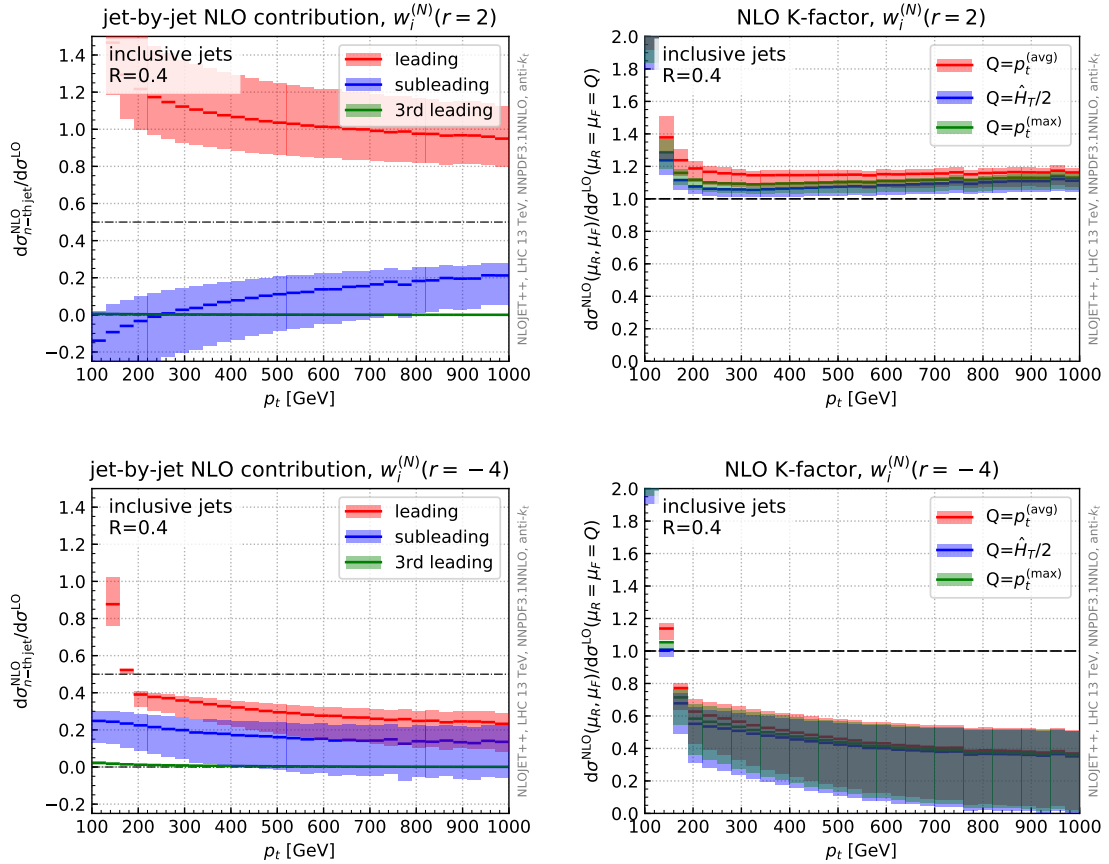
Figure 3. Same as Fig. 1 but using the weighted definitions of type A (see text: jets above p_t^{cut}) for $r = 2$ (top) and $r = -4$ (bottom).

3.2 Weighted (unitary) definitions

We now turn to the study of the weighted (unitary) definitions of the single inclusive-jet cross-section introduced in Sect. 2. We start our discussion with case (A), in which a p_t^{cut} is adopted, and we show that in fact this unitary definition appears to display a somewhat problematic behavior, whose origin is discussed analytically in Sect. 4. We then turn to cases (B) and (C) which provide a natural way to alleviate this problematic behavior.

A. Jets above p_t^{cut}. In Fig. 3 we show again the individual jet contributions and K factor, now using weighted definitions of type (A), with a positive ($r = 2$) and a negative ($r = -4$) value for the exponent in the weights. Note that the K_n, and hence the total K factor, are normalized to the LO weighted jet cross-section which is exactly half of the LO jet cross-section obtained with the standard definition. Indeed, at LO we have $w_1 = w_2 = 1/2$, by kinematic constraint, for the weighted definition, independently of r.

We first discuss the behaviour for p_t far above p_t^{cut}. Broadly speaking, positive weights enhance the difference between leading and second leading jets, with features that resemble those of the standard definition for the individual K_n factors. This is also true, in particular, for the total K factor for p_t sufficiently larger than p_t^{cut} (top row of Fig. 3). Negative values of r, on the other hand, have the effect of balancing the difference between leading and subleading jets. This results in more similar individual K_n factors, at the price of an overall larger total K factor (bottom row of Fig. 3). At very large p_t this effect becomes very large, which can be easily understood as follows: whenever we have three jets passing the p_t cut with $p_{t1,2} \gg p_{t3}$
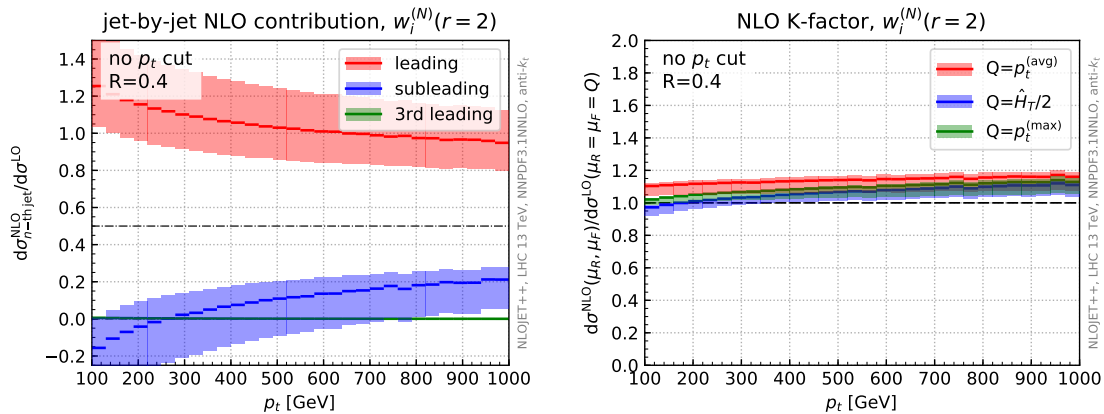
Figure 4. Same as Fig. 1, but using a weighted definition of type B (all jets) for $r = 2$.

we have

$$w_{1,2}^{(3)}(r < 0) = \frac{p_{t1,2}^r}{p_{t1}^r + p_{t2}^r + p_{t3}^r} \sim \left(\frac{p_{t3}}{p_{t1,2}}\right)^{|r|} \ll 1\,, \tag{3.4}$$

$$w_{3}^{(3)}(r < 0) = \frac{p_{t3}^r}{p_{t1}^r + p_{t2}^r + p_{t3}^r} \sim 1\,. \tag{3.5}$$

The contributions of the two leading jets to the inclusive cross-section, which are strongly dominating the NLO cross-section for the standard definition (or for the weighted definition with $r \geq 0$), are now power suppressed by the weights. Furthermore, corresponding virtual corrections have two jets in the final state with $w_{1,2}^{(2)}(r < 0) = 1/2$. At large p_t real and virtual corrections with $p_t^{\text{cut}} \ll p_{t3} \ll p_{t1,2} \sim p_t$ therefore yield, after integration over p_{t3}, a negative contribution enhanced by $\log(p_t/p_t^{\text{cut}})$, corresponding to the large corrections seen in Fig. 3.

Now turning to the region where $p_t \to p_t^{\text{cut}}$, we see from Fig. 3 that this weighted definition (for both positive and negative r) develops a singular behavior. The origin of this behavior is explained analytically in Section 4. For the time being, we note that these singularities, both for $p_t \gg p_t^{\text{cut}}$ and for $p_t \to p_t^{\text{cut}}$, are of logarithmic origin and could in principle be dealt with resummation.

In summary, the weighted definitions of type (A) (with p_t^{cut}) have the undesirable feature of developing problematically unstable behaviors for p_t close to the p_t cut as well as at large p_t for $r < 0$. In the other p_t regions their perturbative behavior now shows large K factors also at NLO since the accidental cancellation of the standard definition is spoiled; while this is perhaps more natural, it does not suggest an improvement in perturbative behavior over the standard definition.

B. All jets. A natural way of curing the logarithmic divergence observed when $p_t \to p_t^{\text{cut}}$ using weights of type (A) is to include all jets down to a p_t much smaller than the first bin of the distribution. Based on Fig. 3, taking a p_t^{cut} two or three times smaller than the first bin of the distribution would already get rid of most of the sensitivity to p_t^{cut}, e.g. without any need for an additional resummation. One can view the weighted definition of type (B) as simply taking the limit $p_t^{\text{cut}} \to 0$ and one should not expect our conclusions to change as long as p_t^{cut} remains much smaller than the first bin of the distribution, say $p_t^{\text{cut}} \sim 20 - 30$ GeV. This possibility is only sensible for positive weights, for which the low p_t part of the spectrum is suppressed. For negative weights this choice is infrared unsafe.

Results are shown in Fig. 4 for $r = 2$. As expected, the singular behavior of the K factor for p_t close to p_t^{cut} is now absent, and features similar to those of the standard definition are now recovered. Specifically, non-overlapping scale variation bands are observed in the low p_t region, though to a smaller extent than in the standard case. As a last comment, we have checked that this definition does not suffer from large non-perturbative corrections, such as those coming from underlying events, despite involving low-p_t jets. In a practical experimental context, one would still need to make sure that this remains true with realistic
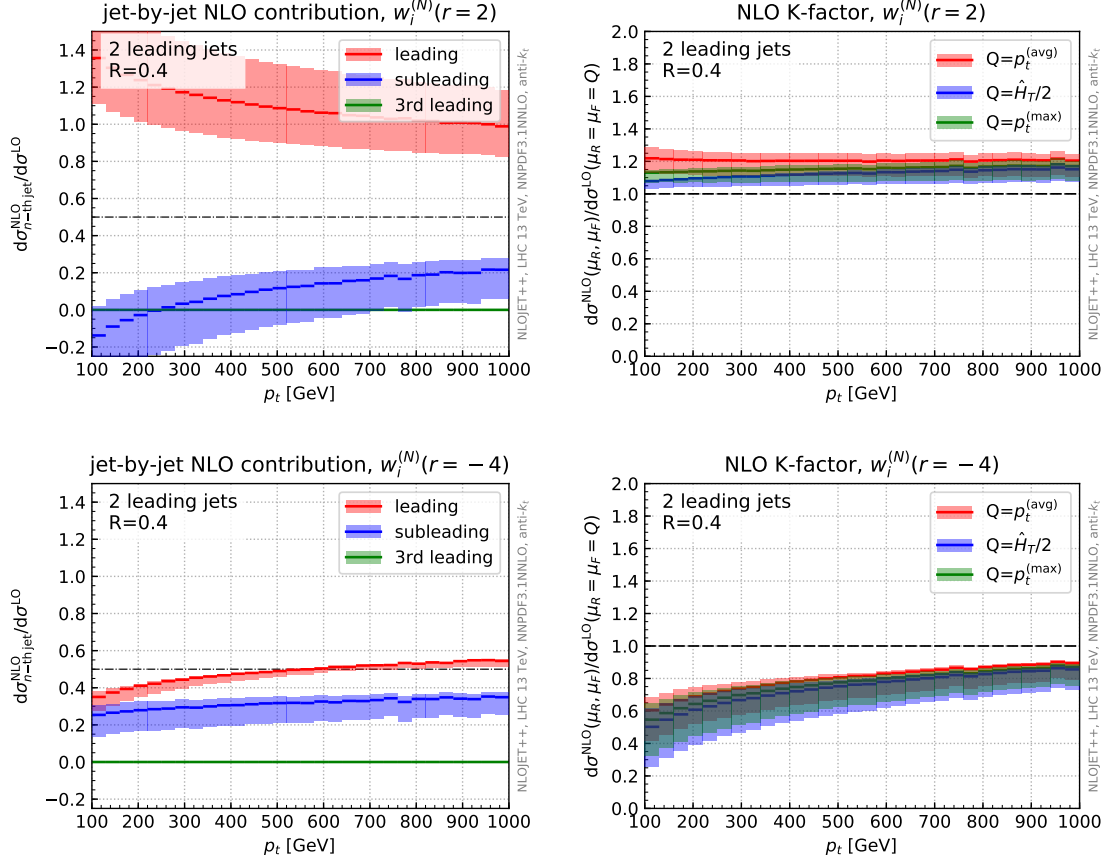
Figure 5. Same as Fig. 1, but using the weighted definitions of type C (two leading jets) for $r = 2$ (top) and $r = -4$ (bottom).

pileup conditions.

C. Two leading jets. An alternative choice, motivated by the observation that the contribution of the third jet to the inclusive jet cross-section is much smaller than that of the first two jets (see Fig. 1) is to switch to definitions of type (C), in which only the two leading jets are included in the weights, whether or not they pass a given $p_t^{\rm cut}$. Clearly this should also remove the problem of the behavior for $p_t \sim p_t^{\rm cut}$ of definitions of type (A). This approach is similar in spirit to what is done when looking at the dijet cross-section. Results in this case are presented in Fig. 5 for the individual K factors K_n and the total K factor. The situation for positive r is again similar to what we observe for the standard definition: in particular there seems to be a large compensation between the leading and subleading jets, leading to a rather flat K factor, though larger than in the standard case.

As explained above, negative values of r have the effect of normalizing the individual K_n factors for the leading and subleading jets, reducing the effect of the compensation seen in the standard case. Furthermore, the uncertainty bands obtained for the three different scale choices now overlap. Nevertheless, the inclusive K factor is relatively larger than for the standard definition and shows a somewhat strong p_t dependence.

Comparing these results to the other weighted definitions, we see that the logarithmic divergence for p_t close to $p_t^{\rm cut}$ which is observed in Fig. 3 when using the jets above $p_t^{\rm cut}$ has now disappeared for both positive and negative r. This, as discussed above, is expected: the weights do not depend on whether one or two of the two leading jets passes the $p_t^{\rm cut}$, so the definition becomes independent of the cut. Furthermore, the issue with large K factors at large p_t for negative r when including jets above $p_t^{\rm cut}$ has also disappeared. This is simply because the third jet no longer contributes to the weights and therefore the large contribution seen in Eq. (3.4) is absent.

In summary, weighted definitions of type (C) behave similarly to the standard definition for positive r. The perturbative behavior for negative r changes, with some desirable features (the individual K factors K_1 and K_2 are similar, and the scale uncertainty bands for different scale choices overlap), and some undesirable ones (the overall K factor is larger).

4 Non-unitarity and perturbative behavior

We now show how several features of the results presented in the previous section can be understood on the basis of simple analytic arguments. Specifically, we show that the behavior in the vicinity of p_t^{cut} is strongly tied to the unitarity, or lack thereof, of the various definitions.

We first provide general (if somewhat formal) arguments, exploiting the fact that at NLO the jet functions used for partitioning the phase-space have a compact and manageable form. We then perform more explicit calculations using a soft and collinear approximation which shows that the effects discussed in Section 3.2 have a simple leading logarithmic origin.

4.1 Dependence on p_t^{cut} and R: a general argument

In order to understand the behavior of various definitions we need an explicit expression for the contribution to the N-jet cross-section $\frac{d\sigma_{N\,\text{jet}}^{(k)}}{dp_t}$ introduced in Eq. (2.7) and to the n-th jet cross-section $\frac{d\sigma_{n\text{-th jet}}^{(k)}}{dp_t}$ introduced in Eq. (2.8). These can be constructed in terms of parton-level cross-sections by introducing explicit jet functions that cluster final-state partons into jets, in the latter case further supplemented by a function that selects the n-th leading jet, and bins the result into a fixed p_t bin. In order to cancel infrared singularities, the k-th order contribution must be constructed by adding up contributions coming from final states with a number of final-state partons that goes from two (with k virtual loops), up to $k + 2$ (with k real emissions on top of the Born level). For instance the NLO $k = 1$ term receives contributions both from a two-parton final state with one loop, and from a real emission three-parton state, and so on.

Explicitly, we can write the N-exclusive jets contribution, Eq. (2.7), as a sum of terms where the N jets are produced from an m parton final-state, $\mathrm{d}\Phi_m$,

$$\frac{\mathrm{d}\sigma_{N\,\text{jets}}^{(k)}}{\mathrm{d}p_t} = \sum_{m=2}^{k+2} \int \mathrm{d}\Phi_m \frac{\mathrm{d}\hat{\sigma}_m^{(k)}}{\mathrm{d}\Phi_m} G_{m \to N\,\text{jets}}(\Phi_m, p_t)\,, \tag{4.1}$$

where $G_{m \to N\,\text{jets}}$ is the jet function which cluster m partons into N jets. $G_{m \to N\,\text{jets}}$ contains the function F_N, Eq. (2.4), which in turn includes the possible weights. The jet function thus depends on the jet momentum p_t, and on the partonic phase space variables $\mathrm{d}\Phi_m$.

We can give an explicit expression of $G_{m \to N}$ at NLO ($k = 1$). For this, let us denote by k_{ti} the parton transverse momenta, with $k_{t1} \geq k_{t2} \geq k_{t3}$. Using the anti-$k_t$ [10] jet clustering with $R < \frac{\pi}{2}$, one has

$$G_{2 \to 1} = G_{2 \to 3} = 0 \tag{4.2}$$

$$G_{2 \to 2} = \Theta(p_t > p_t^{\text{cut}}) \left\{ 2\, w^{(2)}(p_t; p_t, p_t)\, \delta(p_t - k_{t1}) \right\} \tag{4.3}$$

$$G_{3 \to 1} = \Theta(\Delta R_{23} > R)\, \Theta(k_{t1} > p_t^{\text{cut}} > k_{t2} > k_{t3}) \left\{ w^{(1)}(p_t; p_t)\, \delta(p_t - k_{t1}) \right\} \tag{4.4}$$

$$G_{3 \to 2} = \Theta(\Delta R_{23} > R)\, \Theta(k_{t1} > k_{t2} > p_t^{\text{cut}} > k_{t3}) \left\{ \sum_{i=1}^{2} w^{(2)}(p_t; k_{t1}, k_{t2})\, \delta(p_t - k_{ti}) \right\}$$

$$+\, \Theta(\Delta R_{23} < R)\, \Theta(p_t > p_t^{\text{cut}}) \left\{ 2\, w^{(2)}(p_t; p_t, p_t)\, \delta(p_t - k_{t1}) \right\} \tag{4.5}$$

$$G_{3 \to 3} = \Theta(\Delta R_{23} > R)\, \Theta(k_{t1} > k_{t2} > k_{t3} > p_t^{\text{cut}}) \left\{ \sum_{i=1}^{3} w^{(3)}(p_t; k_{t1}, k_{t2}, k_{t3})\delta(p_t - k_{ti}) \right\}, \tag{4.6}$$

where we have defined, as is customary, $\Delta R_{ij} = \sqrt{(\Delta\phi_{ij})^2 + (\Delta y_{ij})^2}$, as the distance between parton i and parton j in the rapidity-azimuth plane, with y and ϕ the rapidity and the azimuthal angle respectively. Note also that, due to momentum conservation, it is sufficient to consider the recombination of the two softest

partons. The second line of Eq. (4.5) corresponds to the case where the two softest partons cluster, yielding two back-to-back jets of momentum k_{t1}.

Using Eqs. (4.2)-(4.6), the issue of unitarity vs. cancellation of the dependence on p_t is easily understood. On the one hand, it is clear that the standard definition is not unitary and only the weighted definitions are unitary because

$$\int \mathrm{d}\, p_t \, G_{3\to 1} + G_{3\to 2} + G_{3\to 3}\big|_{\text{wgt}} = \Theta(k_{t1} > p_t^{\text{cut}})\,, \tag{4.7}$$

This result, valid for any r, means that integrating the single-jet cross-section over p_t yields the total cross-section for producing (at least) one jet above p_t^{cut} (with definitions of type (A) in the sense of Sect. 2) or the total cross-section (for definitions of type (B) or of type (C)). Hence these choices are unitary, and thus the standard choice cannot be.

On the other hand, it is clear that the inclusive cross-section is independent of p_t^{cut} when using the standard definition. Indeed, in this case one has

$$G_{3\to 1}+G_{3\to 2}+G_{3\to 3}\big|_{\text{std}} = \Theta(p_t > p_t^{\text{cut}})\left\{\Theta(\Delta R_{23} > R)\left[\sum_i^3 \delta(p_t - k_{ti})\right]+\Theta(\Delta R_{23} < R)2\,\delta(p_t - k_{t1})\right\}, \tag{4.8}$$

where now the subscript "std" denotes that in the definition of F_N, Eq. (2.4), the standard case in Eq. (2.5) has been selected. The result Eq. (4.8) is manifestly independent of p_t^{cut} since all the dependence on p_t^{cut} is factored in an overall Θ function which is always satisfied as long as one has at least one jet in the event. In practice, the dependence on p_t^{cut} disappears since, when integrating over the partonic transverse momenta, the N-jet contribution has p_t^{cut} as a lower bound of integration while the $N-1$-jet contribution has p_t^{cut} as an upper bound. When summing both contributions, the p_t^{cut} dependence cancels.

When one instead uses a unitary definition which explicitly introduces a p_t^{cut} dependence, such as definition (A), this cancellation is spoiled: whether a jet passes a cut or not changes the weights of all the other jets, thereby introducing a cutoff dependence of the observable. The lack of cancellation then propagates into the individual n-th jet cross-sections, thus explaining the singular behavior observed in Fig. 3 when $p_t \sim p_t^{\text{cut}}$. Of course this cutoff dependence is not present for the two other weighted definitions, (B) and (C), even if the weight associated to a jet still depends on the other jets in the event, which is needed to eventually ensure the unitarity of the cross-section.

We can similarly understand the R dependence or lack thereof of the leading jet contribution, which as discussed in Sect. 3.1 controls the behavior of the NLO K factor, by introducing explicit expressions for individual jet functions. We now need to consider the n-th leading jet contribution, Eq. (2.8)

$$\frac{\mathrm{d}\sigma_{n\text{-th jet}}^{(k)}}{\mathrm{d}p_t} = \sum_{m=2}^{k+2} \int \mathrm{d}\Phi_m \frac{\mathrm{d}\hat{\sigma}_m^{(k)}}{\mathrm{d}\Phi_m} S_{m\to n\text{-th jet}}(\Phi_m, p_t)\,, \tag{4.9}$$

where the functions $S_{m\to n\text{-th jet}}$ are defined summing the contributions coming from the n-th jet in the functions G given above. By direct calculation, we find

$$S_{2\to p_{t1}} = S_{2\to p_{t2}} = \frac{1}{2}\, G_{2\to 2} \tag{4.10}$$

$$\begin{aligned} S_{3\to p_{t1}} = \Theta(p_t > p_t^{\text{cut}})\, \delta(p_t - k_{t1}) &\left\{\Theta(\Delta R_{23} > R)\left[\Theta(p_t^{\text{cut}} > k_{t2} > k_{t3})w^{(1)}(p_t; k_{t1})\right.\right. \\ &\qquad + \Theta(k_{t2} > p_t^{\text{cut}} > k_{t3})\, w^{(2)}(p_t; k_{t1}, k_{t2}) \\ &\qquad \left.+ \Theta(k_{t2} > k_{t3} > p_t^{\text{cut}})w^{(3)}(p_t; k_{t1}, k_{t2}, k_{t3})\right] \\ &\left.+ \Theta(\Delta R_{23} < R)\, w^{(2)}(p_t; p_t, p_t)\right\} \end{aligned} \tag{4.11}$$

$$\begin{aligned} S_{3\to p_{t2}} = \Theta(k_{t1} > p_t > p_t^{\text{cut}})&\left\{\Theta(\Delta R_{23} > R)\, \delta(p_t - k_{t2})\left[\Theta(p_t^{\text{cut}} > k_{t3})\, w^{(2)}(p_t; k_{t1}, k_{t2})\right.\right. \\ &\qquad \left.+ \Theta(k_{t3} > p_t^{\text{cut}})\, w^{(3)}(p_t; k_{t1}, k_{t2}, k_{t3})\right] \end{aligned}$$

$$+ \Theta(\Delta R_{23} < R) \, \delta(p_t - k_{t1}) \, w^{(2)}(p_t; p_t, p_t) \Big\} \tag{4.12}$$

$$S_{3 \to p_{t3}} = \Theta(k_{t1} > k_{t2} > p_t > p_t^{\text{cut}}) \, \delta(p_t - k_{t3}) \, \Theta(\Delta R_{23} > R) \, w^{(3)}(p_t; k_{t1}, k_{t2}, k_{t3}) \,. \tag{4.13}$$

If now one sets all weights $w = 1$, Eq. (4.11) takes the form

$$S_{3 \to p_{t1}}\big|_{\text{std}} = \Theta(p_t > p_t^{\text{cut}}) \, \delta(p_t - k_{t1}) = S_{2 \to p_{t1}}\big|_{\text{std}} \,, \tag{4.14}$$

where the subscript "std" again denotes that in the definition of F_N, Eq. (2.4), the standard case in Eq. (2.5) has been selected. This means that all the Θ functions simplify, leading to an overall factor providing a condition that is always satisfied if at least one jet in the event is above p_t^{cut}. At NLO, the leading jet contribution is therefore always given by the transverse momentum of the hardest parton (this is valid for both the real contribution with three partons in the final state and the virtual corrections with two partons), independently of the jet radius R. Note that, one can similarly see that for any weighted definition, at NLO, corrections to the leading jet are R-dependent for the same reason that the weighted definitions depend on p_t^{cut}: the value of the weights depend on how many partons have $\Delta R_{ij} > R$. Furthermore, the NLO corrections for the subleading and third-leading jet also depend on R. This is trivial for the latter which shows an explicit R dependence in (4.13). For the subleading jet, this is due to the fact that the p_t of the jet changes (between k_{t1} and k_{t2}) depending on how ΔR_{23} compares to R.

4.2 Dependence on p_t^{cut} and R: the soft-collinear approximation

The arguments outlined above may seem somewhat formal. To gain further analytic insight, it is useful to take a soft-collinear approximation in which case Eqs. (4.1),(4.9) simplify considerably. Indeed, if one considers a collinear splitting at a small angle ϑ, the NLO contribution from a real emission can be written in simple form by parametrising the final-state momenta as

$$p_1^\mu = \tilde{p}_a^\mu + \mathcal{O}(k_\perp^2), \quad p_2^\mu = (1-z)\tilde{p}_b^\mu + k_\perp^\mu + \mathcal{O}(k_\perp^2), \quad p_3^\mu = z\,\tilde{p}_b^\mu - k_\perp^\mu + \mathcal{O}(k_\perp^2), \tag{4.15}$$

where $\tilde{p}_a^\mu$ and $\tilde{p}_b^\mu$ are the Born final-state hard directions, z is the longitudinal momentum fraction of the splitting, and the transverse momentum $k_\perp$ satisfies $k_\perp \cdot \tilde{p}_a = k_\perp \cdot \tilde{p}_b = 0$; $k_\perp$ can then be parametrized by the angle ϑ between p_2 and p_3 and an azimuthal angle φ.

Including only terms that produce a logarithmic enhancement in the limit $\vartheta \to 0$, the real emission contribution takes the form

$$d\Phi_3 \frac{d\hat{\sigma}_3^{(1)}}{d\Phi_3} = \sum_{i=q,g} \left[\frac{d\sigma_2^{(0)}}{dp_t}(\tilde{p}_t) \right]_i \left[\frac{\alpha_s C_i}{\pi} P_i(z) \right] \mathrm{d}\tilde{p}_t \, \mathrm{d}z \, \frac{\mathrm{d}\vartheta^2}{\vartheta^2} \frac{d\varphi}{2\pi}. \tag{4.16}$$

Note that within this approximation recoil effects on p_1 become negligible. They could be addressed using a similar formalism but going beyond the small-angle approximation that we adopt here.

In Eq. (4.16) $[d\sigma_2^{(0)}/dp_t]_i$, with $i = q, g$, is the LO differential cross-section for producing a quark or a gluon of transverse momentum $\tilde{p}_t$, correctly normalized in such a way that the sum over i gives the total cross-section. $P_i(z)$ corresponds to the standard Altarelli-Parisi splitting functions with z the momentum fraction of the collinear splitting (see Appendix A for explicit expressions) from which we have explicitly factored out a colour factor $2\,C_i$ ($C_i = C_F$ for quarks and $C_i = C_A$ for gluons). Finally, φ is the azimuthal angle corresponding of the emission with respect to the Born-level parton that splits. At this accuracy, the NLO one-loop virtual correction has exactly the same form as Eq. (4.16) integrated over the full phase-space of the extra real emission, but with the opposite sign. In what follows, we further assume that the extra emission is soft so we can approximate $P_i(z) \approx \frac{1}{z}$. This soft approximation is made for the sake of simplicity and can easily be lifted to include the full splitting function.

The soft-collinear approximation is sufficient to obtain results in fair agreement with the full calculation, and specifically reproduce three important aspects discussed in Sect. 3. First, we can see explicitly how the cancellation of the p_t^{cut} dependence which happens in the standard case is spoiled for the weighted definition (A) and restored with definitions (B) and (C). Second, we are able to identify the R dependence of the second leading jet with out-of-cone radiation. Third, we can further study the impact of weighted definitions

at large p_t. Conversely, working in a soft-collinear approximation, we are neglecting all recoil effects. This means in particular that the calculation below will not reproduce the large K_1 factor for the leading jet. The text below outlines the structure of the calculation and our main results, deferring additional details to Appendix A.

The fact that the real and virtual contributions have the opposite sign implies that the N-jet contribution Eq. (4.1) and the n-th jet contribution Eq. (4.9) take respectively the simple form

$$\frac{d\sigma_{N\,\text{jets}}^{(k)}}{dp_t} \approx \sum_{i=q,g} \frac{C_i}{\pi} \int d\tilde{p}_t \, dz \frac{d\vartheta^2}{\vartheta^2} \left[\frac{d\sigma_2^{(0)}}{dp_t}(\tilde{p}_t) \right]_i \alpha_s P_i(z) \left\{ G_{3\to N\,\text{jets}} - G_{2\to N\,\text{jets}} \right\} \tag{4.17}$$

$$\equiv \sum_{i=q,g} \left[\frac{d\sigma_2^{(0)}}{dp_t}(p_t) \right]_i \frac{C_i}{\pi} \ln\left(\frac{R_{\max}^2}{R^2} \right) I_N \tag{4.18}$$

and

$$\frac{d\sigma_{n\text{-th jet}}^{(k)}}{dp_t} \approx \sum_{i=q,g} \frac{C_i}{\pi} \int d\tilde{p}_t \, dz \frac{d\vartheta^2}{\vartheta^2} \left[\frac{d\sigma_2^{(0)}}{dp_t}(\tilde{p}_t) \right]_i \alpha_s P_i(z) \left\{ S_{3\to n\text{-th jet}} - S_{2\to n\text{-th jet}} \right\} \tag{4.19}$$

$$\equiv \sum_{i=q,g} \left[\frac{d\sigma_2^{(0)}}{dp_t}(p_t) \right]_i \frac{C_i}{\pi} \ln\left(\frac{R_{\max}^2}{R^2} \right) J_n \,, \tag{4.20}$$

where in both cases $R_{\max}$ is the upper limit of the ϑ integration. The functions I_N and J_n can be cast in a simple closed analytic form by writing the LO cross-section as a power law

$$\left[\frac{d\sigma_2^{(0)}}{dp_t}(\tilde{p}_t) \right]_i \sim \frac{1}{\tilde{p}_t^{m_i}}, \tag{4.21}$$

where m_i is, in general, different for the quark and gluon case. In Appendix A explicit analytic expressions are given for the standard definition, with the general definitions easily amenable to numerical treatment.

We can now use Eqs. (4.18),(4.20) to address the issues mentioned above. We start by investigating the behavior in the $p_t \to p_t^{\text{cut}}$ limit and focus on the leading jet. J_1 receives real contributions from $S_{3\to p_{t1}}$, Eq. (4.11), and virtual corrections from $S_{2\to p_{t1}}$, Eq. (4.10). The latter contribution cancels against the real one in the region $\Delta R_{23} \equiv \vartheta < R$. Up to power corrections in z, we can set $k_{t2} = (1-z)k_{t1}$ and $k_{t3} = zk_{t1}$. For $p_t \to p_t^{\text{cut}}$ we can then assume $k_{t3} < p_t^{\text{cut}}$ and we are left with two terms:

$$J_1 \stackrel{p_t \to p_t^{\text{cut}}}{\sim} \int_{1-p_t^{\text{cut}}/p_t}^{p_t^{\text{cut}}/p_t} dz \, P(z) \, w^{(1)}(p_t; p_t) - \int_{1-p_t^{\text{cut}}/p_t}^{p_t^{\text{cut}}/p_t} dz \, P(z) \, w^{(2)}(p_t; p_t, p_t). \tag{4.22}$$

The first term corresponds to $k_{t2} < p_t^{\text{cut}}$ while the second term includes the real emissions with $k_{t2} > p_t^{\text{cut}}$ as well as the remaining virtual corrections. After integration over z, we thus find

$$J_1 = \log\left(\frac{p_t^{\text{cut}}}{p_t - p_t^{\text{cut}}} \right) - \omega \log\left(\frac{p_t^{\text{cut}}}{p_t - p_t^{\text{cut}}} \right) = \begin{cases} 0 & (\text{standard}) \\ -\frac{1}{2} \log\left(\frac{p_t - p_t^{\text{cut}}}{p_t^{\text{cut}}} \right) & (\text{weighted (A)}) \end{cases}, \tag{4.23}$$

where $\omega = 1$ for the standard definition and $\omega = \frac{1}{2}$ for the weighted definition (A), independently of the exponent r which enters the definition of the weights, Eq. (2.4). In the same limit it turns out that J_2 and J_3 are nonsingular. This explains our findings from Sect. 3: the unitary definition suffers from a logarithmic divergence close to p_t^{cut} while the standard definition is independent of the value of p_t^{cut}. Furthermore, this behavior (see Fig. 3), only affects the leading jet, whose properties are encoded in J_1. Of course it also follows from Eq. (4.23) that when $p_t^{\text{cut}} \ll p_t$, corresponding to using definitions of the weights of type (B), the singular behavior disappears. A similar conclusion can be reached for the definition of type (C).

Next, we can also use Eq. (4.20) to predict the small-R behavior of the second and third leading jet contributions. In both cases one would get a logarithmic enhancement at small R. Note that at first sight Eq. (4.20) seems to imply that the leading jet contribution also has a logarithmic R dependence in the
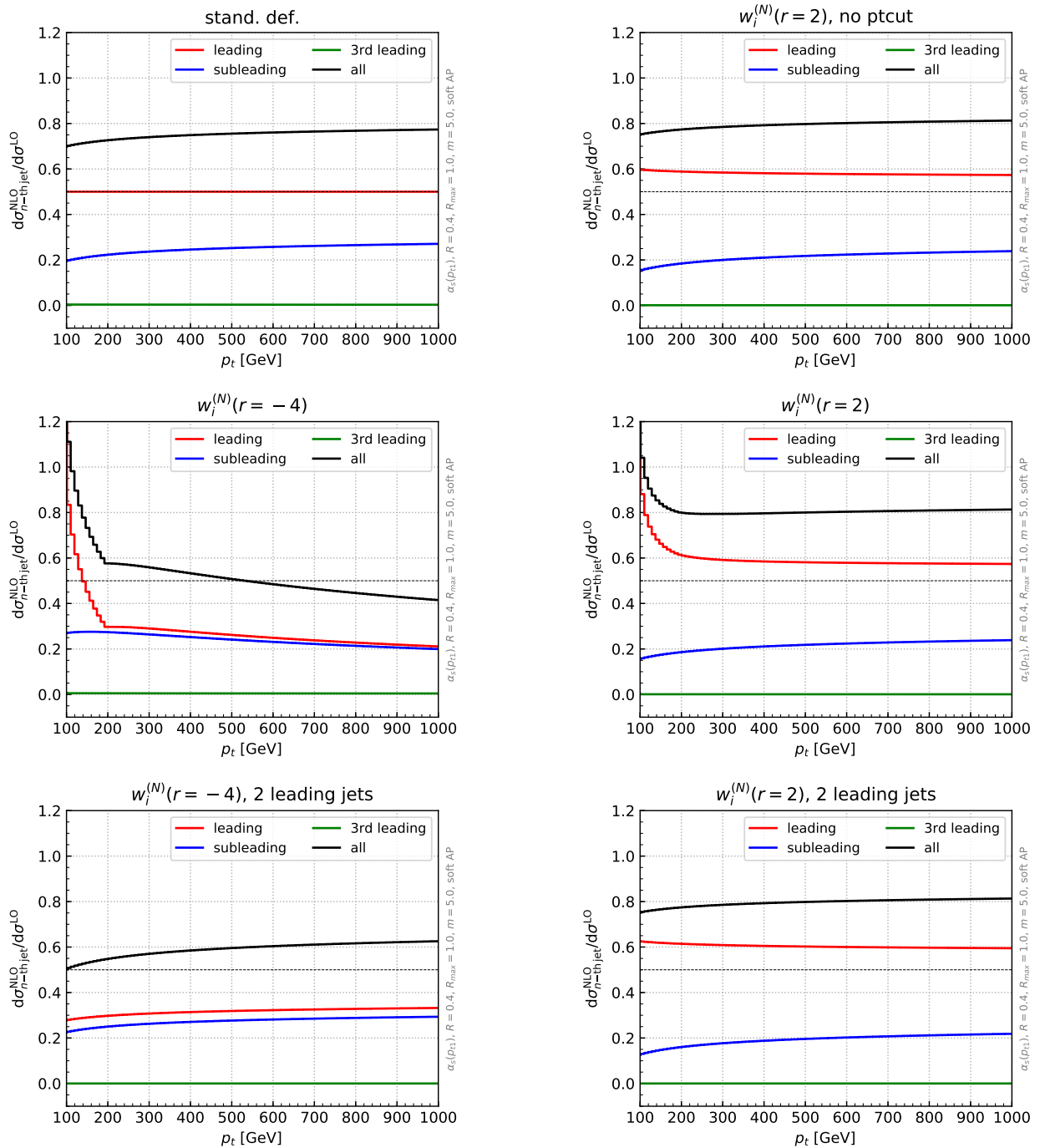
Figure 6. Contributions from the leading, subleading, and third-leading jets to the NLO inclusive K factors in the soft-collinear approximation. The standard definition (top left) is compared to weighted definition of type (B) (no p_t^{cut}) with $r = 2$ (top right), weighted definitions of type (A) (with p_t^{cut}) with $r = -4$ (middle left) and $r = 2$ (middle right) and of type (C) (two jets) also with with $r = -4$ (bottom left) and $r = 2$ (bottom right).

standard case, in contradiction to the behavior observed in Fig. 2, and to our previous general conclusion based on Eq. (4.14). However, one should realise that, in the small-R limit where Eq. (4.20) holds, Eq. (4.23) implies that J_1 is zero, and thus obviously R-independent in the standard case. In all weighted cases J_1 is non-vanishing, and thus the leading jet contribution becomes R-dependent in agreement with our previous analytic and numerical arguments, with a logarithmic dependence on R in the small-R limit.

Finally, we can study the limit of the functions J_n when $p_t \gg p_t^{\mathrm{cut}}$, in the weighted case with r negative

Definition	standard	weighted		
		(A) above p_t^{cut}	(B) all jets	(C) two leading
Reference plot	Fig. 1	Fig. 3	Fig. 4	Fig. 5
unitarity	no	yes	yes	yes
no large logs close to p_t^{cut}	✓	✗	✓	✓
no large logs at large p_t	✓	✓ for $r > 0$ ✗ for $r < 0$	✓	✓
overlapping scale variation bands	✗ ✓ with uncorr. uncert. [4, 12]	✓	✓	✓
no large cancellations between K_1 and K_2	✗	✗	✗	✗ for $r > 0$ ✓ for $r < 0$

Table 1. Summary of the main properties of the various single-inclusive jet definitions studied in this paper.

and $|r| \sim |m_i| \sim 4$. In this case, we find that the contributions from the leading and the subleading jet are comparable (see the Appendix A for details), partially solving the problem of the large compensation seen in the standard definition or for positive values of r, as observed in Sect. 3.2, Fig. 3.

Results obtained for the leading, subleading and third-leading jet contributions using the approximation Eqs. (4.18),(4.20) are shown in Fig. 6 for a representative set of cases, to be compared to Figs. 1,3-5. All plots have been produced implementing Eq. (4.19), with Eq. (4.21) and $m = 5$. Note that this parametrization of the LO p_t spectrum already includes initial state PDFs. We have checked that using the exact LO partonic cross-section yields similar results. We choose $R_{\max} = 1$ and use $R = 0.4$ to allow for a comparison with the full results presented in Section 3. Finally, we set $\alpha_s(p_{t1})$. As anticipated, it is clear that the main qualitative features of the exact results are reproduced by the soft-collinear approximation.

5 Conclusions

In this paper we have addressed the potential issue of the non-unitarity of the single-jet inclusive cross-section, by introducing a series of alternative weighted definitions of this observable which are unitary in the sense that upon integration they lead to the total cross-section. The main features of the various definitions we have considered are summarised in Table 1.

Our conclusion is that a naive weighted approach [type (A) of Sect. 2] in which one simply introduces a weighting of all jets above a certain p_t^{cut} is flawed, in the sense that it develops logarithmic singularities associated with the transverse momentum cut on jets, p_t^{cut}. More sophisticated definitions avoid this problem by setting p_t^{cut} to zero [type (B)] or by considering only the two leading jets [type (C)]. Both these definitions could be more challenging to implement in a practical (experimental) environment.

Additionally, even leaving aside practical considerations, there does not seems to be any real advantage in adopting these definitions in term of perturbative stability. In particular, all weighted definitions with positive r show features at best similar to the standard definition. Furthermore, the apparent perturbative instability of the conventional definition appears in fact to be the manifestation of an unnatural smallness of the NLO K factors which only happens for a limited range of jet radius $R \sim 0.4$. It is a consequence of an accidental cancellation which makes standard scale variation unreliable as a means of estimating missing higher order corrections. This apparent issue for example disappears with more conservative estimates of the perturbative uncertainties.

One possible case of interest is the definition of type (C), focusing on the two leading jets, with $r < 0$. Compared to the standard definition, it has the potential advantage of reducing the large difference between the K factor of the leading and subleading jets, at the cost of having a larger overall NLO K factor.

Our final conclusion is that unitary definitions of the jet inclusive cross-section are at best as good as the standard definition. While the latter shows no critical sign of pathological features, the former are rather more contrived, with no real advantage other than their unitarity which however is per se not causing any perturbative problem.

Acknowledgments

A NLO cross-section in the soft-collinear approximation

The N-jet contribution and the n-th jet contribution to the differential cross-section at NLO in the soft-collinear approximation are given by Eq. (4.17) and Eq. (4.19) respectively. Using an explicit expression for the splitting functions P_i and for the G or the S functions in the collinear limit we can perform the phase-space integration explicitly.

The splitting functions P_i are

$$
\begin{aligned}
P_q(z) &= \sum_{j=q,g} P_{jq} = \frac{1+(1-z)^2}{2z} = \frac{1}{z} + \mathcal{O}(1) \\
P_g(z) &= \sum_{j=q,g} P_{jg} = \frac{1}{2}\left[2\frac{1-z}{z} + z(1-z) + \frac{T_R N_f}{C_A}(z^2+(1-z)^2)\right] = \frac{1}{z} + \mathcal{O}(1)
\end{aligned}
\tag{A.1}
$$

where the $z \leftrightarrow (1-z)$ symmetry has been exploited in such a way that all soft-collinear singularities are at $z = 0$ (see e.g. [15]). Note that a $2C_F$ or $2C_A$ factor, respectively, has been explicitly factored out.

By adopting the parametrization of the final-state given in Eq. (4.15), the jet functions G and S can be rewritten in the collinear and small R limit, i.e. $\Delta R_{23} = \vartheta \leq R \ll 1$. For the weighted definition with jets above p_t^{cut} we have:

$$
G_{2\to1} = G_{2\to3} = 0 \tag{A.2}
$$

$$
G_{2\to2} = \Theta(\tilde{p}_t > p_t^{\text{cut}})w^{(2)}(p_t|\tilde{p}_t,\tilde{p}_t)[\delta(p_t-\tilde{p}_t) + \delta(p_t-\tilde{p}_t)] \tag{A.3}
$$

$$
G_{3\to1} = \Theta(\vartheta^2 > R^2)\Theta(\tilde{p}_t > p_t^{\text{cut}}; z\tilde{p}_t < p_t^{\text{cut}}; (1-z)\tilde{p}_t < p_t^{\text{cut}})w^{(1)}(p_t|\tilde{p}_t)[\delta(p_t-\tilde{p}_t)] \tag{A.4}
$$

$$
\begin{aligned}
G_{3\to2} = &\ \Theta(\vartheta^2 < R^2)\Theta(\tilde{p}_t > p_t^{\text{cut}})w^{(2)}(p_t|\tilde{p}_t,\tilde{p}_t)[\delta(p_t-\tilde{p}_t) + \delta(p_t-\tilde{p}_t)] \\
&+ \Theta(\vartheta^2 > R^2)\Theta(\tilde{p}_t > p_t^{\text{cut}}) \\
&\quad \Big\{\Theta(z\tilde{p}_t < p_t^{\text{cut}}; (1-z)\tilde{p}_t > p_t^{\text{cut}})w^{(2)}(p_t|\tilde{p}_t,(1-z)\tilde{p}_t)[\delta(p_t-\tilde{p}_t) + \delta(p_t-(1-z)\tilde{p}_t)] \\
&\quad + \Theta(z\tilde{p}_t > p_t^{\text{cut}}; (1-z)\tilde{p}_t < p_t^{\text{cut}})w^{(2)}(p_t|\tilde{p}_t,z\tilde{p}_t)[\delta(p_t-\tilde{p}_t) + \delta(p_t-z\tilde{p}_t)]\Big\}
\end{aligned}
\tag{A.5}
$$

$$
\begin{aligned}
G_{3\to3} = &\ \Theta(\vartheta^2 > R^2)\Theta(\tilde{p}_t > p_t^{\text{cut}}; z\tilde{p}_t > p_t^{\text{cut}}; (1-z)\tilde{p}_t > p_t^{\text{cut}}) \\
&\ w^{(3)}(p_t|\tilde{p}_t,z\tilde{p}_t,(1-z)\tilde{p}_t)[\delta(p_t-\tilde{p}_t) + \delta(p_t-z\tilde{p}_t) + \delta(p_t-(1-z)\tilde{p}_t)].
\end{aligned}
\tag{A.6}
$$

and

$$
S_{2\to p_{t1}} = S_{2\to p_{t2}} = \Theta(\tilde{p}_t > p_t^{\text{cut}})w^{(2)}(p_t|\tilde{p}_t,\tilde{p}_t)\delta(p_t-\tilde{p}_t) \tag{A.7}
$$

$$
\begin{aligned}
S_{3\to p_{t1}} = &\ \Theta(\vartheta^2 < R^2)\Theta(\tilde{p}_t > p_t^{\text{cut}})w^{(2)}(p_t|\tilde{p}_t,\tilde{p}_t)\delta(p_t-\tilde{p}_t) + \Theta(\vartheta^2 > R^2) \\
&\ \Big[\Theta(\tilde{p}_t > p_t^{\text{cut}}; z\tilde{p}_t < p_t^{\text{cut}}; (1-z)\tilde{p}_t < p_t^{\text{cut}})w^{(1)}(p_t|\tilde{p}_t)\delta(p_t-\tilde{p}_t) \\
&\ + \Theta(\tilde{p}_t > p_t^{\text{cut}}; z\tilde{p}_t > p_t^{\text{cut}}; (1-z)\tilde{p}_t < p_t^{\text{cut}})w^{(2)}(p_t|\tilde{p}_t,z\tilde{p}_t)\delta(p_t-\tilde{p}_t) \\
&\ + \Theta(\tilde{p}_t > p_t^{\text{cut}}; z\tilde{p}_t < p_t^{\text{cut}}; (1-z)\tilde{p}_t > p_t^{\text{cut}})w^{(2)}(p_t|\tilde{p}_t,(1-z)\tilde{p}_t)\delta(p_t-\tilde{p}_t) \\
&\ + \Theta(\tilde{p}_t > p_t^{\text{cut}}; z\tilde{p}_t > p_t^{\text{cut}}; (1-z)\tilde{p}_t > p_t^{\text{cut}})w^{(3)}(p_t|\tilde{p}_t,z\tilde{p}_t,(1-z)\tilde{p}_t)\delta(p_t-\tilde{p}_t)\Big]
\end{aligned}
\tag{A.8}
$$

$$
\begin{aligned}
S_{3\to p_{t2}} = &\ \Theta(\vartheta^2 < R^2)\Theta(\tilde{p}_t > p_t^{\text{cut}})w^{(2)}(p_t|\tilde{p}_t,\tilde{p}_t)\delta(p_t-\tilde{p}_t) + \Theta(\vartheta^2 > R^2) \\
&\ \Big\{\Theta(\tilde{p}_t > p_t^{\text{cut}}; z\tilde{p}_t > p_t^{\text{cut}}; (1-z)\tilde{p}_t < p_t^{\text{cut}})w^{(2)}(p_t|\tilde{p}_t,z\tilde{p}_t)\delta(p_t-z\tilde{p}_t)
\end{aligned}
\tag{A.9}
$$

$$+ \Theta(\tilde{p}_t > p_t^{\text{cut}}; z\tilde{p}_t < p_t^{\text{cut}}; (1-z)\tilde{p}_t > p_t^{\text{cut}})w^{(2)}(p_t|\tilde{p}_t, (1-z)\tilde{p}_t)\delta(p_t - (1-z)\tilde{p}_t)$$

$$+ \Theta(\tilde{p}_t > p_t^{\text{cut}}; z\tilde{p}_t > p_t^{\text{cut}}; (1-z)\tilde{p}_t > p_t^{\text{cut}})w^{(3)}(p_t|\tilde{p}_t, z\tilde{p}_t, (1-z)\tilde{p}_t)$$

$$[\Theta(z > 1/2)\delta(p_t - z\tilde{p}_t) + \Theta(z < 1/2)\delta(p_t - (1-z)\tilde{p}_t)]\Big\}$$

$$S_{3 \to pt3} = \Theta(\vartheta^2 > R^2)\Theta(\tilde{p}_t > p_t^{\text{cut}}; z\tilde{p}_t > p_t^{\text{cut}}; (1-z)\tilde{p}_t > p_t^{\text{cut}})w^{(3)}(p_t|\tilde{p}_t, z\tilde{p}_t, (1-z)\tilde{p}_t)$$

$$[\Theta(z < 1/2)\delta(p_t - z\tilde{p}_t) + \Theta(z > 1/2)\delta(p_t - (1-z)\tilde{p}_t)] \tag{A.10}$$

The standard definition can trivially be recovered by setting the weights to 1, while the case of the weighted definition including all jets can be obtained by taking the limit $p_t^{\text{cut}} \to 0$. Similarly, the weighted definition with 2 leading jets is instead obtained by firstly taking the limit $p_t^{\text{cut}} \to 0$ and by then keeping the terms proportional to $\delta(p_t - \tilde{p}_t)$ as well as the terms proportional to either $\delta(p_t - z\tilde{p}_t)$ if $z > 1/2$, or $\delta(p_t - (1-z)\tilde{p}_t)$ if $z < 1/2$, modifying the weights accordingly.

The $\tilde{p}_t$ integration in Eqs. (4.17)-(4.19) can be simplified using the delta functions $\delta(p_t - \tilde{p}_t)$, $\delta(p_t - z\tilde{p}_t)$ and $\delta(p_t - (1-z)\tilde{p}_t)$. The ϑ integration leads to a logarithmic dependence on the jet radius R. The only nontrivial integral is over z, thereby leading to a final result of the form of Eqs. (4.18),(4.20). Explicitly, I_N and J_n there present are given by:

$$I_1 = \Theta(p_t < 2p_t^{\text{cut}}) \int_{1-p_t^{\text{cut}}/p_t}^{p_t^{\text{cut}}/p_t} dz\, P(z)\, [1]\, \tilde{\sigma}(p_t) \tag{A.11}$$

$$I_2 = \Theta(p_t < 2p_t^{\text{cut}})\Bigg[\int_{p_t^{\text{cut}}/p_t}^{1} dz\, P(z) \left[\frac{1}{1+z^r}\right] \tilde{\sigma}(p_t)$$

$$+ \int_0^{1-p_t^{\text{cut}}/p_t} dz\, P(z) \left(\left[\frac{1}{1+(1-z)^r}\right]\tilde{\sigma}(p_t) - \left[\frac{1}{2}\right]\tilde{\sigma}(p_t)\right) - \int_{1-p_t^{\text{cut}}/p_t}^{1} dz\, P(z) \left[\frac{1}{2}\right]\tilde{\sigma}(p_t)\Bigg]$$

$$+ \Theta(p_t > 2p_t^{\text{cut}})\Bigg[\int_{1-p_t^{\text{cut}}/p_t}^{1} dz\, P(z) \left[\frac{1}{1+z^r}\right]\tilde{\sigma}(p_t)$$

$$+ \int_0^{p_t^{\text{cut}}/p_t} dz\, P(z) \left(\left[\frac{1}{1+(1-z)^r}\right]\tilde{\sigma}(p_t) - \left[\frac{1}{2}\right]\tilde{\sigma}(p_t)\right) - \int_{p_t^{\text{cut}}/p_t}^{1} dz\, P(z) \left[\frac{1}{2}\right]\tilde{\sigma}(p_t)\Bigg] \tag{A.12}$$

$$+ \int_{p_t/(p_t+p_t^{\text{cut}})}^{1} dz\, P(z) \left[\frac{z^r}{1+z^r}\right]\frac{1}{z}\tilde{\sigma}\left(\frac{p_t}{z}\right)$$

$$+ \int_0^{p_t^{\text{cut}}/(p_t+p_t^{\text{cut}})} dz\, P(z) \left(\left[\frac{(1-z)^r}{1+(1-z)^r}\right]\frac{1}{1-z}\tilde{\sigma}\left(\frac{p_t}{1-z}\right) - \left[\frac{1}{2}\right]\tilde{\sigma}(p_t)\right)$$

$$- \int_{p_t^{\text{cut}}/(p_t+p_t^{\text{cut}})}^{1} dz\, P(z) \left[\frac{1}{2}\right]\tilde{\sigma}(p_t)$$

$$I_3 = \Theta(p_t > 2p_t^{\text{cut}}) \int_{p_t^{\text{cut}}/p_t}^{1-p_t^{\text{cut}}/p_t} dz\, P(z) \left[\frac{1}{1+z^r+(1-z)^r}\right]\tilde{\sigma}(p_t)$$

$$+ \int_0^{p_t/(p_t+p_t^{\text{cut}})} dz\, P(z) \left[\frac{z^r}{1+z^r+(1-z)^r}\right]\frac{1}{z}\tilde{\sigma}\left(\frac{p_t}{z}\right) \tag{A.13}$$

$$+ \int_{p_t^{\text{cut}}/(p_t+p_t^{\text{cut}})}^{1} dz\, P(z) \left[\frac{(1-z)^r}{1+z^r+(1-z)^r}\right]\frac{1}{1-z}\tilde{\sigma}\left(\frac{p_t}{1-z}\right)$$

$$J_1 = \Theta(p_t < 2p_t^{\text{cut}}) \left[\int_{1-p_t^{\text{cut}}/p_t}^{p_t^{\text{cut}}/p_t} dz\, P(z)\, [1]\, \tilde{\sigma}(p_t) - \int_{1-p_t^{\text{cut}}/p_t}^{1} dz\, P(z) \left[\frac{1}{2} \right] \tilde{\sigma}(p_t) \right.$$

$$+ \int_0^{1-p_t^{\text{cut}}/p_t} dz\, P(z) \left(\left[\frac{1}{1+(1-z)^r} \right] \tilde{\sigma}(p_t) - \left[\frac{1}{2} \right] \tilde{\sigma}(p_t) \right) + \int_{p_t^{\text{cut}}/p_t}^{1} dz\, P(z) \left[\frac{1}{1+z^r} \right] \tilde{\sigma}(p_t) \right]$$

$$+ \Theta(p_t > 2p_t^{\text{cut}}) \left[\int_{p_t^{\text{cut}}/p_t}^{1-p_t^{\text{cut}}/p_t} dz\, P(z) \left[\frac{1}{1+z^r+(1-z)^r} \right] \tilde{\sigma}(p_t) - \int_{p_t^{\text{cut}}/p_t}^{1} dz\, P(z) \left[\frac{1}{2} \right] \tilde{\sigma}(p_t) \right.$$

$$\left. + \int_0^{p_t^{\text{cut}}/p_t} dz\, P(z) \left(\left[\frac{1}{1+(1-z)^r} \right] \tilde{\sigma}(p_t) - \left[\frac{1}{2} \right] \tilde{\sigma}(p_t) \right) + \int_{1-p_t^{\text{cut}}/p_t}^{1} dz\, P(z) \left[\frac{1}{1+z^r} \right] \tilde{\sigma}(p_t) \right]$$

$$\text{(A.14)}$$

$$J_2 = \int_{p_t/(p_t+p_t^{\text{cut}})}^{1} dz\, P(z) \left[\frac{z^r}{1+z^r} \right] \frac{1}{z} \tilde{\sigma}\left(\frac{p_t}{z} \right) - \int_{p_t^{\text{cut}}/(p_t+p_t^{\text{cut}})}^{1} dz\, P(z) \left[\frac{1}{2} \right] \tilde{\sigma}(p_t)$$

$$+ \int_0^{p_t^{\text{cut}}/(p_t+p_t^{\text{cut}})} dz\, P(z) \left(\left[\frac{(1-z)^r}{1+(1-z)^r} \right] \frac{1}{1-z} \tilde{\sigma}\left(\frac{p_t}{1-z} \right) - \left[\frac{1}{2} \right] \tilde{\sigma}(p_t) \right)$$

$$+ \int_{1/2}^{p_t/(p_t+p_t^{\text{cut}})} dz\, P(z) \left[\frac{z^r}{1+z^r+(1-z)^r} \right] \frac{1}{z} \tilde{\sigma}\left(\frac{p_t}{z} \right)$$

$$+ \int_{p_t^{\text{cut}}/(p_t+p_t^{\text{cut}})}^{1/2} dz\, P(z) \left[\frac{(1-z)^r}{1+z^r+(1-z)^r} \right] \frac{1}{1-z} \tilde{\sigma}\left(\frac{p_t}{1-z} \right)$$

$$\text{(A.15)}$$

$$J_3 = \int_0^{1/2} dz\, P(z) \left[\frac{z^r}{1+z^r+(1-z)^r} \right] \frac{1}{z} \tilde{\sigma}\left(\frac{p_t}{z} \right) + \int_{1/2}^{1} dz\, P(z) \left[\frac{(1-z)^r}{1+z^r+(1-z)^r} \right] \frac{1}{1-z} \tilde{\sigma}\left(\frac{p_t}{1-z} \right)$$

$$\text{(A.16)}$$

where the terms in squared brackets correspond to the weights, here given for a definition of type (A), and we have set the running coupling scale to $p_t^{\max} \equiv p_{t1} = \tilde{p}_t$ and introduced

$$\tilde{\sigma}(x) \equiv \frac{d\sigma_2^{(0)}}{dp_t}(x)\, \alpha_s(x). \qquad \text{(A.17)}$$

In the fixed coupling approximation or if we take $\alpha_s(p_t)$, the coupling can be factorized out of the integration and directly moved to Eq. (4.18) or Eq. (4.20). Note that the above expressions do not assume $z \ll 1$. Keeping the full z dependence of the splitting functions would therefore account for hard-collinear splittings.

In the general weighted case, these integrals can only be computed numerically. Results for the standard (unweighted) definition are found by simply removing all terms in square brackets. In this case, by using Eq. (4.21) for the Born cross-section and the soft approximation of the splitting functions these integrals can be computed exactly in the fixed coupling approximation and their expressions are

$$I_1^{(\text{std})} = \Theta(p_t < 2p_t^{\text{cut}}) \ln\left(\frac{p_t^{\text{cut}}}{p_t - p_t^{\text{cut}}} \right) \qquad \text{(A.18)}$$

$$I_2^{(\text{std})} = \Theta(p_t > 2p_t^{\text{cut}}) \ln\left(\frac{p_t^{\text{cut}}}{p_t - p_t^{\text{cut}}} \right) - \Theta(p_t < 2p_t^{\text{cut}}) \ln\left(\frac{p_t^{\text{cut}}}{p_t - p_t^{\text{cut}}} \right) + \ln\left(\frac{p_t^{\text{cut}}}{p_t + p_t^{\text{cut}}} \right) \qquad \text{(A.19)}$$

$$+ \frac{1}{m-1}\left(1 - \left(\frac{p_t + p_t^{\text{cut}}}{p_t} \right)^{1-m} \right) - (m-1)\left(\frac{p_t^{\text{cut}}}{p_t+p_t^{\text{cut}}} \right)\, {}_3F_2\left(1,1,2-m;2,2; \frac{p_t^{\text{cut}}}{p_t+p_t^{\text{cut}}} \right)$$

$$I_3^{(\text{std})} = -\Theta(p_t > 2p_t^{\text{cut}}) \ln\left(\frac{p_t^{\text{cut}}}{p_t - p_t^{\text{cut}}} \right) - \ln\left(\frac{p_t^{\text{cut}}}{p_t + p_t^{\text{cut}}} \right) \qquad \text{(A.20)}$$

$$+ \frac{1}{m-1}\left(\frac{p_t+p_t^{\text{cut}}}{p_t} \right)^{1-m} - H_{m-1} + (m-1)\left(\frac{p_t^{\text{cut}}}{p_t+p_t^{\text{cut}}} \right)\, {}_3F_2\left(1,1,2-m;2,2; \frac{p_t^{\text{cut}}}{p_t+p_t^{\text{cut}}} \right)$$

and

$$J_1^{(\text{std})} = 0 \tag{A.21}$$

$$J_2^{(\text{std})} = -\frac{1}{2}(m-1)\,_3F_2\left(1,1,2-m;2,2;\frac{1}{2}\right) - \frac{2^{1-m}-1}{m-1} - \log 2 \tag{A.22}$$

$$J_3^{(\text{std})} = \frac{1}{2}(m-1)\,_3F_2\left(1,1,2-m;2,2;\frac{1}{2}\right) - H_{m-1} + \frac{2^{1-m}}{m-1} + \log 2 \tag{A.23}$$

where H_n are harmonic numbers, $_pF_q$ is a generalized hypergeometric function, and m is the power of the LO cross-section in Eq. (4.21), which can in principle differ for quarks and gluons.

Adding up all contributions we get:

$$\begin{aligned}
\frac{d\sigma^{(k)}}{dp_t} &= \sum_{i=q,g}\left[\frac{d\sigma_2^{(0)}}{dp_t}(p_t)\right]_i \frac{\alpha_s C_i}{\pi}\ln\left(\frac{R_{\max}^2}{R^2}\right)(I_1+I_2+I_3)^{(\text{std})} \\
&= \sum_{i=q,g}\left[\frac{d\sigma_2^{(0)}}{dp_t}(p_t)\right]_i \frac{\alpha_s C_i}{\pi}\ln\left(\frac{R_{\max}^2}{R^2}\right)(J_1+J_2+J_3)^{(\text{std})} \\
&= \sum_{i=q,g}\left[\frac{d\sigma_2^{(0)}}{dp_t}(p_t)\right]_i \frac{\alpha_s C_i}{\pi}\ln\left(\frac{R_{\max}^2}{R^2}\right)\left[\frac{1}{m_i-1} - H_{m_i-1}\right].
\end{aligned} \tag{A.24}$$

For $m_q = m_g$, the K factor is flat, since both the p_t and the p_t^{cut} dependence have canceled completely in the square bracket in the last line. The only remaining dependence on p_t would therefore come either from differences between the quark and gluon contributions ($m_q \neq m_g$) or from the running of α_s which was neglected in the above result.

We conclude by studying the large p_t limit of J_n in the weighted case. When $p_t \to \infty$, from Eqs. (A.14)-(A.15) we get

$$J_1^{(\text{wgt})} \overset{p_t\to\infty}{\sim} -\int_0^1 dz\,P(z)\left[\frac{1}{2}\right]\tilde{\sigma}(p_t) + \int_0^1 dz\,P(z)\left[\frac{1}{1+z^r+(1-z)^r}\right]\tilde{\sigma}(p_t) \tag{A.25}$$

$$\begin{aligned}
J_2^{(\text{wgt})} \overset{p_t\to\infty}{\sim} &-\int_0^1 dz\,P(z)\left[\frac{1}{2}\right]\tilde{\sigma}(p_t) \\
&+ \int_{1/2}^1 dz\,P(z)\left[\frac{z^r}{1+z^r+(1-z)^r}\right]\frac{1}{z}\tilde{\sigma}\left(\frac{p_t}{z}\right) \\
&+ \int_0^{1/2} dz\,P(z)\left[\frac{(1-z)^r}{1+z^r+(1-z)^r}\right]\frac{1}{1-z}\tilde{\sigma}\left(\frac{p_t}{1-z}\right)
\end{aligned} \tag{A.26}$$

while J_3 in Eq. (A.16) does not depend on p_t and it is always negligible. Assuming that the LO cross-section behaves accordingly to the power law Eq. (4.21), and choosing a negative exponent $r \sim -m$ for the weights, it appears that J_1 and J_2 become the same in the $p_t \to \infty$ limit. Hence, the effect of the weight is to balance the leading and the second leading jet contributions.

References

[1] A. D. Martin, R. G. Roberts, and W. J. Stirling, *Structure Function Analysis and psi, Jet, W, Z Production: Pinning Down the Gluon*, Phys. Rev. **D37** (1988) 1161.

[2] F. Aversa, P. Chiappetta, M. Greco, and J. P. Guillet, *Higher Order Corrections to QCD Jets*, Phys. Lett. **B210** (1988) 225.

[3] S. D. Ellis, Z. Kunszt, and D. E. Soper, *The One Jet Inclusive Cross-section at Order α_s^3: Gluons Only*, Phys. Rev. Lett. **62** (1989) 726.

[4] J. Currie, E. W. N. Glover, and J. Pires, *Next-to-Next-to Leading Order QCD Predictions for Single Jet Inclusive Production at the LHC*, Phys. Rev. Lett. **118** (2017), no. 7 072002, [arXiv:1611.01460].

[5] J. Currie, A. Gehrmann-De Ridder, T. Gehrmann, E. W. N. Glover, A. Huss, and J. Pires, *Infrared sensitivity of single jet inclusive production at hadron colliders*, *JHEP* **10** (2018) 155, [arXiv:1807.03692].

[6] Z. Nagy, *Next-to-leading order calculation of three jet observables in hadron hadron collision*, *Phys. Rev.* **D68** (2003) 094002, [hep-ph/0307268].

[7] Z. Nagy, *Three jet cross-sections in hadron hadron collisions at next-to-leading order*, *Phys. Rev. Lett.* **88** (2002) 122003, [hep-ph/0110315].

[8] **NNPDF** Collaboration, R. D. Ball et al., *Parton distributions from high-precision collider data*, *Eur. Phys. J.* **C77** (2017), no. 10 663, [arXiv:1706.00428].

[9] A. Buckley, J. Ferrando, S. Lloyd, K. Nordström, B. Page, M. Rüfenacht, M. Schönherr, and G. Watt, *LHAPDF6: parton density access in the LHC precision era*, *Eur. Phys. J.* **C75** (2015) 132, [arXiv:1412.7420].

[10] M. Cacciari, G. P. Salam, and G. Soyez, *The anti-k_t jet clustering algorithm*, *JHEP* **04** (2008) 063, [arXiv:0802.1189].

[11] M. Cacciari, G. P. Salam, and G. Soyez, *FastJet User Manual*, *Eur. Phys. J.* **C72** (2012) 1896, [arXiv:1111.6097].

[12] M. Dasgupta, F. A. Dreyer, G. P. Salam, and G. Soyez, *Inclusive jet spectrum for small-radius jets*, *JHEP* **06** (2016) 057, [arXiv:1602.01110].

[13] M. Cacciari, S. Frixione, M. L. Mangano, P. Nason, and G. Ridolfi, *The t anti-t cross-section at 1.8-TeV and 1.96-TeV: A Study of the systematics due to parton densities and scale dependence*, *JHEP* **04** (2004) 068, [hep-ph/0303085].

[14] J. Bellm et al., *Jet cross sections at the LHC and the quest for higher precision*, arXiv:1903.12563.

[15] S. Marzani, G. Soyez, and M. Spannowsky, *Looking inside jets: an introduction to jet substructure and boosted-object phenomenology*, arXiv:1901.10342.